

Electrostatically Embedded Many-Body Expansion for Neutral and Charged Metalloenzyme Model Systems

Elbek K. Kurbanov, Hannah R. Leverentz, Donald G. Truhlar, and Elizabeth A. Amin*

Department of Medicinal Chemistry, Department of Chemistry, and Minnesota Supercomputing Institute, University of Minnesota, Minneapolis, Minnesota 55414, United States

S Supporting Information

ABSTRACT: The electrostatically embedded many-body (EE-MB) method has proven accurate for calculating cohesive and conformational energies in clusters, and it has recently been extended to obtain bond dissociation energies for metal–ligand bonds in positively charged inorganic coordination complexes. In the present paper, we present four key guidelines that maximize the accuracy and efficiency of EE-MB calculations for metal centers. Then, following these guidelines, we show that the EE-MB method can also perform well for bond dissociation energies in a variety of neutral and negatively charged inorganic coordination systems representing metalloenzyme active sites, including a model of the catalytic site of the zinc-bearing anthrax toxin lethal factor, a popular target for drug development. In particular, we find that the electrostatically embedded three-body (EE-3B) method is able to reproduce conventionally calculated bond-breaking energies in a series of pentacoordinate and hexacoordinate zinc-containing systems with an average absolute error (averaged over 25 cases) of only 0.98 kcal/mol.

Zinc is an essential transition metal required for the catalytic and structural activity of many enzymes,¹ and it participates in a number of key biological processes in living systems, including immune function,^{2,3} protein synthesis,^{2,5} wound healing,^{4,7} DNA synthesis,^{2,6} and cell division.^{2,6} Zinc metalloenzymes carry out essential functions in a wide variety of biochemical pathways and have attracted much attention as drug design targets; examples include the anthrax toxin lethal factor,⁸ insulin, phosphotriesterase, the matrix metalloproteinases, cytidine deaminase, histone deacetylases, zinc-finger proteins, and human carbonic anhydrase. In these enzymes, zinc may play structural and/or catalytic roles, with catalysis taking place in the first coordination shell.⁹ *In silico* techniques have generally proven valuable for rational drug design and enzyme modeling; however, reliable representation of zinc and other transition metal centers in macromolecules is nontrivial due to the complexity of the coordination environment and charge distribution at the catalytic center. Accurate zinc modeling requires quantum mechanical electronic structure calculations that pose challenges due to system size and the complexity of the calculations. Enabling accurate simulations on large and computationally demanding systems such as biozinc metallic coordination sites is a central focus of quantum chemistry research, and attempts have been made^{9–11} to assess the accuracy of various QM-based strategies for Zn model systems representing biocenters and other complex environments such as nanoparticles and clusters. Fragmentation is a useful strategy for addressing these roadblocks, and various schemes have been explored in order to reduce calculation complexity.^{12–24} The electrostatically embedded many-body expansion (EE-MB) method has emerged as a particularly promising approach.^{10,17,25–29} As described in our previous work,^{10,17,25–30} EE-MB addresses the challenge of system size by partitioning larger complexes into a series of fragments, embedding fragment energies in a field of point charges and running calculations in parallel.

In the EE-MB method,^{10,17,25–30} the fragments into which a system is partitioned are called monomers. In the present study, we examine two variants of this method: the electrostatically embedded pairwise additive (EE-PA) approximation and the electrostatically embedded three-body (EE-3B) approximation. In the former, the energy of systems composed of monomers m , n , p , ... is approximated as

$$E^{\text{PA}} = E^{(1)} + \Delta E^{(2)} \quad (1)$$

where

$$E^{(1)} = \sum_m E_m \quad (2)$$

$$\Delta E^{(2)} = \sum_m \sum_{n > m} \Delta E_{mn}^{(2)} \quad (3)$$

$$\Delta E_{mn}^{(2)} = E_{mn} - E_m - E_n \quad (4)$$

whereas the EE-3B energy is defined as

$$E^{3\text{B}} = E^{\text{PA}} + \Delta E^{(3)} \quad (5)$$

where

$$\Delta E^{(3)} = \sum_m \sum_{n > m} \sum_{p > n} \Delta E_{mnp} \quad (6)$$

$$\Delta E_{mnp} = E_{mnp} - E_{mnp}^{\text{PA}} \quad (7)$$

where E_m , E_{mn} , and E_{mnp} are the energies of a monomer, dimer, and trimer, respectively, embedded in a field of point charges

Received: September 12, 2011

Published: November 29, 2011

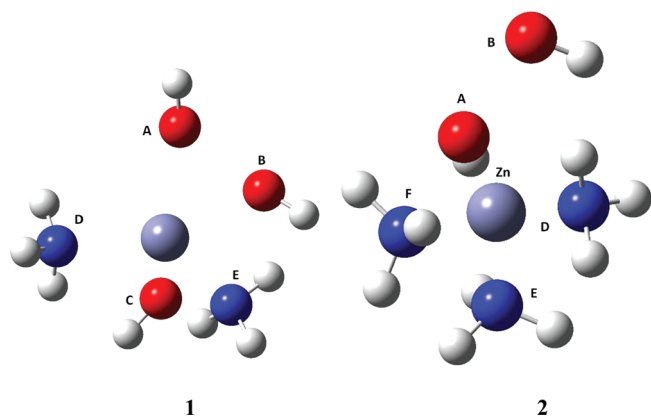


Figure 1. Structures of truncated model Zn biocenter complexes: (1) the anthrax toxin lethal factor active site (LF; 1PWU.pdb),²⁶ $[\text{Zn}(\text{NH}_3)_2(\text{OH})_3]^-$, and (2) matrix metalloproteinase-3 (MMP-3, stromelysin-1; 1SLN.pdb),²⁷ $[\text{Zn}(\text{NH}_3)_3(\text{OH})_2]$. In both cases, histidine residues are represented by ammonias (NH_3), and Glu residues and zinc-binding group (ZBG) oxygens in the cocrystallized inhibitors are represented by hydroxyls (OH^-).

representing the other monomers, and the individual energies are obtained using any type of electronic structure theory.

We have already shown that the EE-MB method can be used to calculate usefully accurate bond dissociation energies at low computational cost for positively charged Zn^{2+} systems; in particular the EE-3B method predicts bond energies obtained by conventional full-system calculations done at the same level of theory to within 1.0 kcal/mol for those cationic Zn^{2+} complexes.³⁰ In the present work, we recommend a set of specific fragmentation strategies to enhance the accuracy of EE-MB for coordination chemistry, and we assess the suitability of the EE-3B method for the more challenging neutral and negatively charged penta- and hexacoordinate Zn systems of biological importance. We also present EE-PA results for comparison.

Charges are calculated for each fragment at the geometry of that monomer in the overall system. For example, if we are calculating the energy of ZnABCDEF , where A, B, C, D, E, and F are ligands, and if one of the fragments is ZnBC , we calculate the partial atomic charges of ZnBC by removing A, D, E, and F from the system. Here, we calculate charges using Merz–Kollman (MK) electrostatic fitting,³⁷ as in previous work on Zn compounds.³⁰

All calculations were done with the M05-2X density functional³¹ and the B2 basis set,⁹ which is a polarized valence-triple- ζ basis set optimized and validated for use with Zn-containing complexes including biozinc coordination systems. Our earlier published work on a variety of Zn–ligand systems of importance in biology, nanotechnology, and drug design^{9,34} showed that incorporating relativistic effects on core electrons significantly increased the accuracy of geometric and energetic calculations for Zn coordination complexes; in the current study, we therefore replaced the 10 innermost electrons of Zn with the (MEFIT, R) relativistic effective core potential.^{32,33} The M05-2X/B2 density functional/basis set combination was chosen because of previous evaluations^{9,34} that yielded very accurate results for zinc complexes. We note explicitly, however, that the main objective of using DFT in this study is to assess whether the EE-MB approximation can reproduce full (unfragmented) calculations. If so, one could, for example, use the EE-MB approximation with

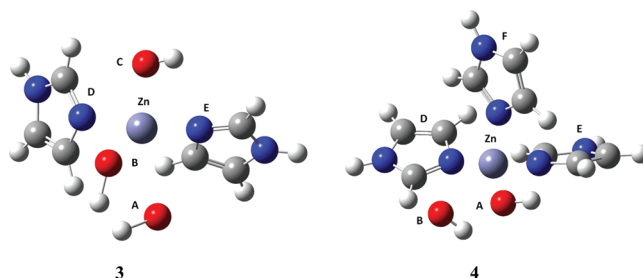


Figure 2. Structures of extended Zn biocenter complexes: (3) the anthrax toxin lethal factor active site (LF; 1PWU.pdb),²⁶ $[\text{Zn}(\text{Imd})_2(\text{OH})_3]^-$, and (4) matrix metalloproteinase-3 (MMP-3, stromelysin-1; 1SLN.pdb),²⁷ $[\text{Zn}(\text{Imd})_3(\text{OH})_2]$. In both cases, histidine residues are represented by imidazoles (Imd), and Glu residues and zinc-binding group (ZBG) oxygens in the cocrystallized inhibitors are represented by hydroxyls (OH^-).

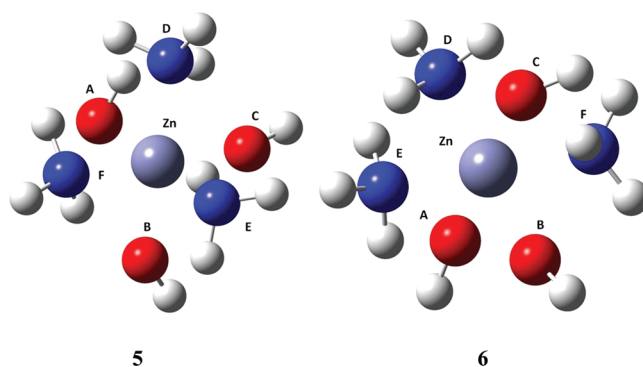


Figure 3. Structures of two octahedral, hexacoordinate Zn complexes ($[\text{Zn}(\text{NH}_3)_3(\text{OH})_3]^-$): (5) *fac* isomer and (6) *mer* isomer.

coupled cluster calculations on the fragments to approximate full coupled cluster calculations that are currently unaffordable.

All unfragmented calculations were performed using *Gaussian 09*.³⁵ All EE-MB calculations were carried out using MBPAC 2011–2,³⁶ an in-house software package that allows the user to define a particular fragmentation scheme and then accesses a locally modified version of *Gaussian 09* to perform the necessary monomer, dimer, and trimer calculations.

In the current work, we consider four pentacoordinate and two hexacoordinate Zn systems. The pentacoordinate complexes are model compounds based on experimental X-ray structures of two Zn metalloenzyme active sites relevant to biology and to the drug design process: the anthrax toxin lethal factor (LF; PDB ID: 1PWU)³⁸ and the matrix metalloproteinase-3 (MMP-3) catalytic site (PDB ID: 1SLN).³⁹ In LF, the catalytic Zn is coordinated by two histidines and one glutamic acid, and in 1PWU, the zinc is also ligated by two oxygens in the hydroxamate zinc-binding group (ZBG) of the cocrystallized inhibitor, forming the complete pentacoordinate system. In MMP-3, the catalytic zinc is similarly coordinated by three histidine residues, and in 1SLN, the two remaining coordination sites are occupied by the carboxylate ZBG of the cocrystallized inhibitor. We specifically chose pentacoordinate systems that include ligands from potential drug scaffold ZBGs, in order to test the ability of EE-MB to reproduce bond dissociation energies that would parallel the interactions of small molecules with drug-target catalytic centers.

We created two simple and two extended models of each biocenter, where the simple models **1** and **2** (Figure 1) represent His residues by ammonias and Glu side chains and ZBG oxygens by hydroxyls, yielding $[\text{Zn}(\text{NH}_3)_2(\text{OH})_3]^-$ as a model for the anthrax toxin lethal factor and $[\text{Zn}(\text{NH}_3)_3(\text{OH})_2]$ as a model for MMP-3. In the extended models **3** and **4** (Figure 2), the ammonias are replaced by full imidazole moieties while the hydroxyls are retained. The hexacoordinate complexes examined here are the *fac* and *mer* isomers of $[\text{Zn}(\text{NH}_3)_3(\text{OH})_3]^-$ (systems **5** and **6**, respectively, Figure 3). In total, these systems comprise four negatively charged and two neutral complexes. For systems **1**–**4**, all Zn–ligand distances were fixed at their experimental X-ray values. The hydrogen atoms on all NH_3 and OH ligands, and all Zn–ligand distances in systems **5** and **6**, were placed at standard distances and default orientations by the *GaussView*⁴⁰ program. The default N–H bond length in NH_3 is 1.00 Å. The default O–H distance is 0.96 Å. For systems **5** and **6**, the default Zn– NH_3 bond length is 1.95 Å, and the default Zn–OH distance is 1.91 Å. Default bond angles for ligand geometries in *GaussView* are obtained through AM1 optimizations. All structures are provided in the Supporting Information.

The quantity we calculate is a relative bond dissociation energy, which is defined as the energy to remove one of the ligands from the coordination system. As discussed in previous work,³⁰ this quantity is the sum of the energies of the two products (separated frozen fragments) minus the energy of the reactant, without including vibrational energy (thus, it is D_e , not D_0). When calculating the energies of a given dissociation product, the embedding charges of the other product are not included because the other product is considered to be infinitely separated.

After performing extensive calculations with various fragmentation schemes on systems **1** and **2**, we established four key fragmentation guidelines that, when applied, yielded the best results for all six systems in the current work. Next, we present these four guidelines.

First, our calculations on neutral and negatively charged Zn systems demonstrate, consistently with our previous findings,³⁰ that one must choose a fragmentation scheme where one of the monomers is Zn^{2+} coordinated to at least two ligands. We rationalize this rule in terms of partial atomic charges. In particular, the charge on unligated or monoligated Zn and even on biligated Zn is much larger than the charge on polyligated Zn; thus fragments consisting of unligated, monoligated, or—to a lesser extent—biligated Zn would not be representative of a portion of a larger system. But if each fragment already has two ligands on Zn, then even in dimers there are three ligands on Zn.

Second, as a corollary to rule 1, we do not dissociate bonds within fragments, as that would result in a product with Zn connected to a single ligand.

Third, at most, one fragment can be charged. We rationalize rule 3 as eliminating the longest-range electrostatic effects.

Finally, our fourth guideline allows no *trans* coordination; i.e., Zn^{2+} cannot be coordinated within a fragment with two ligands that are *trans* to each other. This rule can be understood as requiring links to be compact, although its origin is purely empirical at present.

We use the labeling scheme defined by Figures 1–3, in which A, B, and C (when present) are negatively charged hydroxyl ligands and D, E, and F (when present) are neutral ligands. A consequence of rule 3 for the present study is that Zn^{2+} coupled

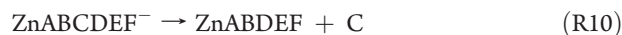
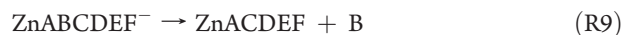
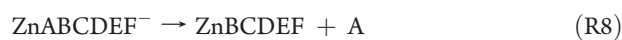
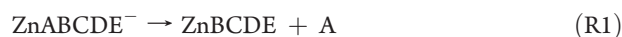
Table 1. Systems Considered in This Work and the Largest Fragment in Each^a

full system	largest fragment
$[\text{Zn}(\text{NH}_3)_2(\text{OH})_3]^-$	$\text{Zn}(\text{OH})_2$ (ZnBC)
$[\text{Zn}(\text{NH}_3)_2(\text{OH})_3]^-$	$\text{Zn}(\text{OH})_2$ (ZnAB)
$[\text{Zn}(\text{NH}_3)_2(\text{OH})_3]^-$	$\text{Zn}(\text{OH})_2$ (ZnBC, ZnAB)
$[\text{Zn}(\text{NH}_3)_3(\text{OH})_2]$	$\text{Zn}(\text{OH})_2$ (ZnAB)
$[\text{Zn}(\text{Imd})_2(\text{OH})_3]^-$	$\text{Zn}(\text{OH})_2$ (ZnBC)
$[\text{Zn}(\text{Imd})_2(\text{OH})_3]^-$	$\text{Zn}(\text{OH})_2$ (ZnAB)
$[\text{Zn}(\text{Imd})_2(\text{OH})_3]^-$	$\text{Zn}(\text{OH})_2$ (ZnBC, ZnAB)
$[\text{Zn}(\text{Imd})_3(\text{OH})_2]$	$\text{Zn}(\text{OH})_2$ (ZnAB)
<i>fac</i> isomer of $[\text{Zn}(\text{NH}_3)_3(\text{OH})_3]^-$	$\text{Zn}(\text{OH})_2$ (ZnBC)
<i>fac</i> isomer of $[\text{Zn}(\text{NH}_3)_3(\text{OH})_3]^-$	$\text{Zn}(\text{OH})_2$ (ZnAC)
<i>fac</i> isomer of $[\text{Zn}(\text{NH}_3)_3(\text{OH})_3]^-$	$\text{Zn}(\text{OH})_2$ (ZnAB)
<i>fac</i> isomer of $[\text{Zn}(\text{NH}_3)_3(\text{OH})_3]^-$	$\text{Zn}(\text{OH})_2$ (ZnAB, ZnBC, ZnAC)
<i>mer</i> isomer of $[\text{Zn}(\text{NH}_3)_3(\text{OH})_3]^-$	$\text{Zn}(\text{OH})_2$ (ZnBC)
<i>mer</i> isomer of $[\text{Zn}(\text{NH}_3)_3(\text{OH})_3]^-$	$\text{Zn}(\text{OH})_2$ (ZnAB)
<i>mer</i> isomer of $[\text{Zn}(\text{NH}_3)_3(\text{OH})_3]^-$	$\text{Zn}(\text{OH})_2$ (ZnAB, ZnBC)

^a When there is more than one row for a given system, it is because the largest fragment is not the same in all calculations on that system.

with two hydroxyl groups must be part of the fragmentation scheme in all six complexes.

Rules 3 and 4, taken together, forbid applying EE-MB to the dissociation of monomer B in **1** or monomer B in **6** because rule 3 would then require Zn to be coordinated within a fragment to ligands A and C in **1** and to ligands A and C in **6**, which in both cases would violate rule 4. After eliminating these processes that cannot be treated by the guidelines, we consider all of the remaining processes, which may be classified as follows:



Keeping the four guidelines in mind, we considered dissociation processes R1–R4 for systems **1** and **3**, processes R5–R7 for

Table 2. Benchmark Bond Energies (kcal/mol)

reaction	system	dissociated bond	bond energy	largest Zn fragment(s) in rxn
R1	1	Zn–A	35.12	ZnBC
R2	1	Zn–C	70.22	ZnAB
R3	1	Zn–D	19.32	ZnBC, ZnAB
R4	1	Zn–E	15.89	ZnBC, ZnAB
R5	2	Zn–D	–5.28	ZnAB
R6	2	Zn–E	–13.49	ZnAB
R7	2	Zn–F	6.19	ZnAB
R1	3	Zn–A	12.03	ZnBC
R2	3	Zn–C	57.01	ZnAB
R3	3	Zn–D	17.51	ZnBC, ZnAB
R4	3	Zn–E	20.68	ZnBC, ZnAB
R5	4	Zn–D	20.3	ZnAB
R6	4	Zn–E	–7.26	ZnAB
R7	4	Zn–F	9.53	ZnAB
R8	5	Zn–A	10.47	ZnBC
R9	5	Zn–B	9.18	ZnAC
R10	5	Zn–C	10.47	ZnAB
R11	5	Zn–D	–15.25	ZnAB, ZnBC, ZnAC
R12	5	Zn–E	–22.28	ZnAB, ZnBC, ZnAC
R13	5	Zn–F	–20.74	ZnAB, ZnBC, ZnAC
R8	6	Zn–A	26.98	ZnBC
R10	6	Zn–C	34.78	ZnAB
R11	6	Zn–D	–15.65	ZnAB, ZnBC
R12	6	Zn–E	–17.64	ZnAB, ZnBC
R13	6	Zn–F	–10.05	ZnAB, ZnBC

Table 3. Unsigned Errors in Bond Energies (kcal/mol) for Systems 1 and 3

	EE-PA		EE-3B	
	1	3	1	3
R1	6.47	4.60	0.85	0.85
R2	6.81	8.71	0.78	1.24
R3	4.62	1.67	0.82	1.01
R4	1.38	4.01	0.81	1.04
mean	4.82	4.75	0.82	1.03

systems 2 and 4, and processes R8–R13 for systems 5 and 6, except for system 6, where process R9 was not considered because it would result in a monomer with ligands A and C positioned *trans* to each other. All systems considered in this work, together with the largest fragment in each, are listed in Table 1.

Benchmark values for bond dissociation energies were obtained by full single-point calculations, i.e., without using the many-body approximation (see Table 2). Note that both the benchmark and the many-body calculations employ the same M05-2X/B2/MEFIT/R method. We measure “errors” as the deviation of the EE-MB results from the full calculations with the same method. If the error is small, then we assume that the method could be used with confidence for systems where full calculations on the entire system are impractically expensive or undoable, either due to system size (larger ligands, entire

Table 4. Unsigned Errors in Bond Energies (kcal/mol) for Systems 2 and 4

	EE-PA		EE-3B	
	2	4	2	4
R5	2.37	5.84	1.10	0.81
R6	5.41	5.57	1.09	0.85
R7	1.91	5.91	1.08	0.83
mean	3.23	5.77	1.09	0.83

Table 5. Unsigned Errors in Bond Energies (Kcal/mol) for Systems 5 and 6

	EE-PA		EE-3B	
	5	6	5	6
R8	8.80	6.57	0.59	1.38
R9	9.26		0.37	
R10	8.73	7.54	0.05	2.20
R11	4.51	3.06	1.44	0.16
R12	4.49	2.40	1.40	1.00
R13	4.32	2.53	1.54	1.30
mean ^a	6.68	4.42	0.90	1.21

^a Mean unsigned error for the five or six cases in the given column.

metalloenzymes) or due to using a higher level of electronic structure theory, for example, coupled cluster theory.

Tables 3, 4, and 5 show the EE-MB bond-breaking energies and mean unsigned errors for all six systems. The systems are quite different, but the performance of the EE-3B method is uniformly good. For example, for 1, the bond dissociation energies range from 16 to 70 kcal/mol, but the error of the EE-3B method is in the range 0.78–0.85 kcal/mol for all four cases. The EE-3B method has a mean unsigned error (MUE) in bond dissociation energy of 0.82 kcal/mol for system 1, 1.09 kcal/mol for system 2, 1.03 kcal/mol for system 3, and 0.83 kcal/mol for system 4. It is encouraging that the EE-3B method performs very well for both the “truncated” model systems 1 and 2 and the “extended” model systems 3 and 4. The MUEs in bond dissociation energies for the hexacoordinate systems 5 and 6 are comparable to those for the pentacoordinate systems, at 0.90 and 1.21 kcal/mol, respectively. As expected, the EE-PA method is less accurate, resulting in MUEs in bond dissociation energies ranging from 3.23 to 6.68 kcal/mol for the systems studied here. Altogether, there are 25 cases in Tables 3, 4, and 5, and averaging the unsigned errors over all 25 gives an overall mean unsigned error of 5.10 kcal/mol for the EE-PA method but only 0.98 kcal/mol for the EE-3B method.

The EE-3B method, when applied using our fragmentation guidelines, reliably yields bond dissociation energies within 1.21 kcal/mol of full-calculation DFT benchmark values, further demonstrating its utility and accuracy for neutral and negatively charged bioinorganic structures, in addition to the positively charged systems evaluated in our previous work. Moreover, EE-MB exhibits high accuracy for “extended” active site models with His residues represented by full imidazole rings rather than ammonias, and for hexacoordinate Zn complexes, indicating its particular usefulness for larger metalloprotein active site systems for which full, high-level electronic structure calculations might

be intractable or may incur a high computational cost. Finally, EE-MB is likely to find use in the drug discovery process; it performs very well for pentacoordinate systems representing a small-molecule drug lead coordinated to a catalytic metal center (which are otherwise quite challenging to model), and it can also be used to obtain key parameters such as bond dissociation energies that can be imported into molecular mechanics force fields to increase the accuracy of simpler and less costly calculations on macromolecular drug targets.

■ ASSOCIATED CONTENT

S Supporting Information. Cartesian coordinates for all Zn systems addressed in this study. This material is available free of charge via the Internet at <http://pubs.acs.org>.

■ AUTHOR INFORMATION

Corresponding Author

*E-mail: eamin@umn.edu.

Notes

The authors declare no competing financial interest.

■ ACKNOWLEDGMENT

The authors express their appreciation to Bo Wang for helpful discussions. This work was supported in part by the National Institutes of Health (R01 AI083234 to E.A.A.), by the University of Minnesota Department of Medicinal Chemistry, and the University of Minnesota Supercomputing Institute for Advanced Computational Research. This work was also supported in part by NSF Grant No. CHE09-56776.

■ REFERENCES

- (1) Sandstead, H. H. *J. Lab. Clin. Med.* **1994**, *124*, 322–327.
- (2) Prasad, A. S. *Nutrition* **1995**, *11*, 93.
- (3) Solomons, N. W. *Nutr. Rev.* **1998**, *56*, 27–28.
- (4) Heyneman, C. A. *Ann. Pharmacotherapy* **1996**, *30*, 186–187.
- (5) MacDonald, R. S. *J. Nutr.* **2000**, *130*, 1500S–1508S.
- (6) Wallwork, J. C.; Duerre, J. A. *J. Nutr.* **1985**, *115*, 252–262.
- (7) Henkin, R. I. *N. Engl. J. Med.* **1974**, *291*, 675–676.
- (8) Chiu, T. L.; Solberg, J.; Patil, S.; Geders, T. W.; Zhang, X.; Rangarajan, S.; Francis, R.; Finzel, B. C.; Walters, M. A.; Hook, D. J.; Amin, E. A. *J. Chem. Inf. Model.* **2009**, *49*, 2726–2734.
- (9) Amin, E. A.; Truhlar, D. G. *J. Chem. Theory Comput.* **2008**, *4*, 75.
- (10) Sorkin, A.; Dahlke, E. E.; Truhlar, D. G. *J. Chem. Theory Comput.* **2008**, *4*, 683.
- (11) Brothers, E. N.; Suarez, D.; Deerfield, D. W., II; Merz, K. M., Jr. *J. Comput. Chem.* **2004**, *25*, 1677.
- (12) Mayhall, N. J.; Raghavachari, K. *J. Chem. Theory Comput.* **2011**, *7*, 1336–1343.
- (13) Zhang, D. W.; Zhang, J. Z. H. *J. Chem. Phys.* **2003**, *119*, 3599.
- (14) Fedorov, D. G.; Kitaura, K. *J. Phys. Chem. A* **2004**, *120*, 6832.
- (15) Li, S.; Li, W.; Fang, T. *J. Am. Chem. Soc.* **2005**, *127*, 7215.
- (16) Bettens, R. P. A.; Lee, A. M. *J. Phys. Chem. A* **2006**, *110*, 8777.
- (17) Dahlke, E. E.; Truhlar, D. G. *J. Chem. Theory Comput.* **2007**, *3*, 46.
- (18) Collins, M. A.; Deev, V. A. *J. Chem. Phys.* **2006**, *125*, 104104.
- (19) Fedorov, D. G.; Kitaura, K. *J. Phys. Chem. A* **2007**, *111*, 6904.
- (20) Hirata, S.; Yagi, K. *Chem. Phys. Lett.* **2008**, *464*, 123.
- (21) Xie, W.; Song, L.; Truhlar, D. G.; Gao, J. *J. Chem. Phys.* **2008**, *128*, 234108.
- (22) Gordon, M. S.; Mullin, J. M.; Pruitt, S. R.; Roskop, L. B.; Slipchenko, L. V.; Boatz, J. A. *J. Phys. Chem. B* **2009**, *113*, 9646.

- (23) Söderhjelm, P.; Aquilante, F.; Ryde, U. *J. Phys. Chem. B* **2009**, *113*, 11085.
- (24) Li, W.; Piecuch, P. *J. Phys. Chem. A* **2010**, *114*, 6721.
- (25) Dahlke, E. E.; Truhlar, D. G. *J. Chem. Theory Comput.* **2007**, *3*, 1342.
- (26) Dahlke, E. E.; Leverentz, H. R.; Truhlar, D. G. *J. Chem. Theory Comput.* **2008**, *4*, 33.
- (27) Dahlke, E. E.; Truhlar, D. G. *J. Chem. Theory Comput.* **2008**, *4*, 1.
- (28) Leverentz, H. R.; Truhlar, D. G. *J. Chem. Theory Comput.* **2009**, *5*, 1573.
- (29) Speetzen, E. D.; Leverentz, H. R.; Lin, H.; Truhlar, D. G. In *Accurate Condensed Phase Electronic Structure Theory*; Manby, F., Ed.; CRC Press: Boca Raton, FL, 2010.
- (30) Hua, D.; Leverentz, H. R.; Amin, E. A.; Truhlar, D. G. *J. Chem. Theory Comput.* **2011**, *7*, 251–255.
- (31) Zhao, Y.; Truhlar, D. G. *Theor. Chem. Acc.* **2008**, *120*, 215–241. Erratum: **2008**, *119*, 525.
- (32) Dolg, M.; Wedig, U.; Stoll, H.; Preuss, H. *J. Chem. Phys.* **1987**, *86*, 866.
- (33) Kaupp, M.; Stoll, H.; Preuss, H. *J. Comput. Chem.* **1990**, *11*, 1029.
- (34) Sorkin, A.; Amin, E. A.; Truhlar, D. G. *J. Chem. Theory Comput.* **2009**, *5*, 1254.
- (35) Frisch, M. J.; Trucks, G. W.; Schlegel, H. B.; Scuseria, G. E.; Robb, M. A.; Cheeseman, J. R.; Scalmani, G.; Barone, V.; Mennucci, B.; Petersson, G. A.; Nakatsuji, H.; Caricato, M.; Li, X.; Hratchian, H. P.; Izmaylov, A. F.; Bloino, J.; Zheng, G.; Sonnenberg, J. L.; Hada, M.; Ehara, M.; Toyota, K.; Fukuda, R.; Hasegawa, J.; Ishida, M.; Nakajima, T.; Honda, Y.; Kitao, O.; Nakai, H.; Vreven, T.; Montgomery, J. A., Jr.; Peralta, J. E.; Ogliaro, F.; Bearpark, M.; Heyd, J. J.; Brothers, E.; Kudin, K. N.; Staroverov, V. N.; Kobayashi, R.; Normand, J.; Raghavachari, K.; Rendell, A.; Burant, J. C.; Iyengar, S. S.; Tomasi, J.; Cossi, M.; Rega, N.; Millam, N. J.; Klene, M.; Knox, J. E.; Cross, J. B.; Bakken, V.; Adamo, C.; Jaramillo, J.; Gomperts, R.; Stratmann, R. E.; Yazyev, O.; Austin, A. J.; Cammi, R.; Pomelli, C.; Ochterski, J. W.; Martin, R. L.; Morokuma, K.; Zakrzewski, V. G.; Voth, G. A.; Salvador, P.; Dannenberg, J. J.; Dapprich, S.; Daniels, A. D.; Farkas, Ö.; Foresman, J. B.; Ortiz, J. V.; Cioslowski, J.; Fox, D. J. *Gaussian 09*, Revision A.01; Gaussian, Inc.: Wallingford, CT, 2009.
- (36) Dahlke, E. E.; Lin, H.; Leverentz, H.; Truhlar, D. G. *MBPAC 2011–2*; University of Minnesota: Minneapolis, MN, 2011.
- (37) Besler, B. H.; Merz, K. M., Jr.; Kollman, P. A. *J. Comput. Chem.* **1990**, *11*, 431.
- (38) Turk, B. E.; Wong, T. Y.; Schwarzenbacher, R.; Jarrell, E. T.; Leppla, S. H.; Collier, J.; Liddington, R. C.; Cantley, L. C. *Nat. Struct. Mol. Biol.* **2003**, *11*, 60–66.
- (39) Becker, J. W.; Marcy, A. I.; Rokosz, L. L.; Axel, M. G.; Burbaum, J. J.; Fitzgerald, P. M. D.; Cameron, P. M.; Esser, C. K.; Hagmann, W. K.; Hermes, J. D.; Springer, J. P. *Protein Sci.* **1995**, *4*, 1966–1976.
- (40) Dennington, R.; Keith, T.; Millam, J. Semichem Inc.: Shawnee Mission, KS, 2009.

■ NOTE ADDED AFTER ASAP PUBLICATION

This paper was published on the Web on December 2, 2011, with missing grant information. The corrected version was reposted on December 30, 2011.